

Finite element approach to simulate performance of multiple-opening reinforced concrete beams

Harith Al-Salman¹, Yasar Ameer Ali², Firas F Hassan³, Mustafa Amoori Kadhim⁴

¹ Department of Civil Engineering, Collage of Engineering, University of Babylon, Babil, Iraq

² Building and Construction Techniques Engineering Department, Al-Mustaqbal University College, Babylon, Iraq

³ Civil Technologies Department, Institute of technology- Baghdad, Middle Technical University, Baghdad, Iraq

⁴ College of engineering, university of Kerbala, Karbala, Iraq

ABSTRACT

This paper presents a comparison designed to manipulate performance characteristics of ten reinforced concrete beams with and without openings under a single monotonic maximum stress at mid-span, depending on the configuration and size of the openings, using the ABAQUS/CAE finite element approach package. The cross-section, arrangement, and opening sizes of all the beams were identical to those of the test beams. The goal of the experimental comparison was to check that all simulation processes were proper and adequate. The numerical analysis results showed that in terms of the failure load, there was a 94 percent agreement between experimentally tested and numerical analysis results. In addition, it was shown that concentrated shear stresses at the corners of the openings causing the failure of the posts between the openings. The numerical study revealed that the influence of increasing main longitudinal steel reinforcement by 28% and 44% more efficient to enhance the ultimate load capacity by rates of 7.61% and 9.61%, respectively, compared to increasing the compressive strength of the beams by 24 %, which led to increasing the ultimate load capacity by 3.72%. Therefore, From the standpoint of difficulty and timesaving, the finite element approach is a very dependable technique for investigating the nonlinear behavior of beams with many apertures.

Keywords: Finite element modelling, reinforced concrete beam, multiple openings, Abaqus.

Corresponding Author:

Harith Al-Salman
Department of Civil Engineering
Collage of Engineering
University of Babylon, Babil, Iraq
E-mail: Harithsama@yahoo.com

1. Introduction

Opening in beams occurs often in practice to provide suitable passage of electrical cable and mechanical ducts. The practical benefit of reinforced concrete beams with openings is the decrease of floor heights owing to utilities passing through the beam rather than beneath it, and the construction benefit is the reduction of the structure's dead weight, resulting in an efficient design. These types of beams with various holes can assist alleviate these issues, and they're especially useful in towering multi-story structures. As a result, a finite element approach can be considered as an accurate analysis tool for simulating these types of beams with openings. ABAQUS CAE package was used in the study; it is a powerful approach for engineering simulation depending on finite element analysis. It can analyze either simple linear or complex nonlinear issues and multi-physics problems. For inelastic behavior used concrete damage plasticity (CDP), it is the general capability to model to represent inelastic behavior of concrete, the concept of isotropic damage elasticity with isotropic tensile and compressive plasticity was used [1, 2]. Since the 1960s, researchers have been studying the behavior

of reinforced concrete beams with apertures in the literature [3, 4, 5, 6, 7]. Al Shaarba et al [8] evaluated experimental results with a three-dimensional nonlinear finite element model for several types of reinforced concrete beams with big gaps under flexural behavior. Compressive strength, the amount of tensile longitudinal steel reinforcement, and the size of the apertures were all factors in the investigation. The load-deflection curves and the load of failure were found to be in good agreement. In addition, the computational study discovered that increasing the compressive strength of concrete and tensile steel reinforcement increases ultimate load capacity but increasing the size of holes decreases ultimate load capacity. H. Madkour and K. Ahmed [9] provided three-dimensional nonlinear elastic damage theory simulations of reinforced concrete beams with apertures. It was more concerned with simulating these beams on a thermodynamic basis. After verifying numerous numerical simulations and considering the nonlinear elastic behavior of the concrete material, a nonlinear concrete model under monotonic static loading was presented (deteriorated state).

The results were compared to experimental data in the literature, and there was a lot of consistency. N.K. Okaili and A.H. Shammari [10] employed a Three-Dimensional finite element analysis approach (ANSYS 12.1) to model fifteen T-section web openings with one incremental concentrated load at the mid-span. It used finite element analysis to verify three experimental T-section beams from the literature. The diameter of circular apertures (50, 70, 90, and 130 mm), the number of web openings (four or six), and the forms of openings were also studied (equivalent square or rhombus openings in area to the circular openings). The main conclusion revealed that for beams with circular holes of diameter equals, a little effect on ultimate load capacity occurred. If the diameter of apertures is equal to or greater than 30% of the web depth, the ultimate load capacity is reduced by at least 21%. Furthermore, the results showed that beams with rhombus web openings had a higher ultimate load capacity than the other two designs (circular and square), whereas beams with circular web openings have a higher ultimate load capacity than beams with square web openings. Using finite element analysis, Shubbar et al [11] quantitatively studied the structural behavior of reinforced concrete beams having circular holes of various sizes and locations (ABAQUS software). Under three-point loading, seven reinforced concrete beams were simulated. In comparison to the control, increasing the size of the holes decreased the load of failure and increased maximum deflection.

When compared to the control beam, the presence of opening has a greater influence in the shear zone, resulting in an increase in maximum deflection ranging from 4% to 22% and a decrease in ultimate load capacity ranging from 26% to 36%. In the flexure zone, however, the existence of opening has less of an effect, resulting in an increase in maximum deflection and a decrease in ultimate load capacity that ranged from 1.5 to 19.7% and 6 to 13%, respectively, when compared to the control beam. The best site for the opening was found to be in the flexure zone of the beam, with a diameter of less than 30% of the beam depth. El-Kashif [12] used a numerical simulation to simulate 39 reinforced concrete beams with holes of less than four inches. The size and shape of the apertures (circular or square), the width of the post, and the shear RFT value were all addressed in the parameter research. It was determined that raising the width of the post, the shear RFT value, and decreasing the size of the opening increases the ultimate load capacity. Furthermore, beams with circular holes offer a higher ultimate load capacity than beams with square openings. As a result, a mathematical formula was developed to estimate the ultimate load capacity of beams having apertures. M. A. J. Hassan and A. F. Izzet [13] computationally investigated thirteen reinforced concrete gable roof beams with apertures under one monotonic focused load at mid-span using finite element analysis (package ABAQUS version 2018). The dimensions of the openings, as well as their configurations and sizes, were studied. It was compared to experimental data and found to be very similar in terms of load versus deflection and crack patterns.

The major findings revealed that, in comparison to experimental results, the average deflection and load of the failure were 1.04 and 0.98, respectively. As a result, from the standpoint of complexity and timesaving, a finite element approach can be used to simulate nonlinear behavior of reinforced concrete gable roof beams with apertures. This paper aims to verify the results obtained in the experimental work often reinforced concrete

beams with multiple openings previously in the study of H.A.Khalaf and A.F.Izzet in terms of a load of failure and ultimate deflection. It also shows the distribution of stresses and strains, as well as the effect of increasing concrete compressive strength and main longitudinal steel reinforcement on the flexure behavior of those beams.

2. Experimental work

Ten reinforced concrete beams with apertures of (2700 mm length x 100 mm width x 400 mm depth) were cast and tested as a simply supported beam under a single contracted load at mid-span, including a reference solid beam with no openings and nine beams with multiple openings. The beams with openings were divided into three groups based on the configuration and size of the openings. Three alternative forms were used for the holes: rectangle, parallelogram, and round. Figures 1 and 2 exhibit steel reinforcing details, whereas Table 1 displays experimental beam details. All beams with apertures were reinforced with four 12 mm and 6 mm diameter bars in the lower and upper chords, respectively, with short stirrups of 4 mm diameter at 50 mm spacing, and shear stirrups at the beam's margins were 6 mm diameter bar at 100 mm spacing. Figure 2 shows a beam post reinforced with four 6 mm bars and coupled with 4 mm steel wire placed 50 mm apart.

According to [14] and [15], three cubes of 150 mm were used to determine the cubic compressive strength of the concrete (f_{cu}), and three cylinders of (150x300 mm) were used to determine the splitting tensile strength of the concrete. The compressive strength of cubic to cylindrical concrete (f'_c) was adjusted using the factor, according to [16]. (0.82). The compressive and tensile strengths of the concrete were determined using an average of three specimens. The steel reinforcement specimens were evaluated using [17]. (4, 6, and 12 mm). All beams were evaluated as a simply supported beam under one concentrated load at mid-span using a hydraulic jack and a load cell with a capacity of 300 kN. The deflection of the beam was manually recorded using a dial gauge with a resolution of 0.01 mm/div and a modest load increment of 2.45 kN. Figure 3 shows a schematic representation of the test.

Table 1. Details of the experimental groups

Name of Group	Number of openings	Shape of openings	Dimensions of openings (mm)	Area of openings(mm^2)	Beam Mark
			Depth x width		
Solid beam	non	without	BS
Group I	10	Rectangular	130 x 102	13260	BR130
		Parallelogram	130 x 102	13260	BT130
		Circular	Dim. 130	13273	BC130
Group II	8	Rectangular	150 x 118	17700	BR150
		Parallelogram	150 x 118	17700	BT150
		Circular	Dim. 150	17671	BC150
Group III	8	Rectangular	175 x 138	24150	BR175
		Parallelogram	175 x 138	242150	BT175
		Circular	Dim. 175	24053	BC175

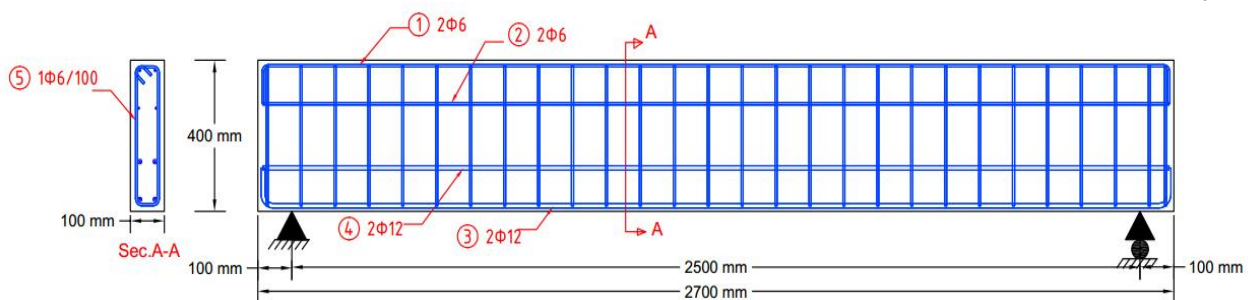


Figure 1. Details of reference solid beam

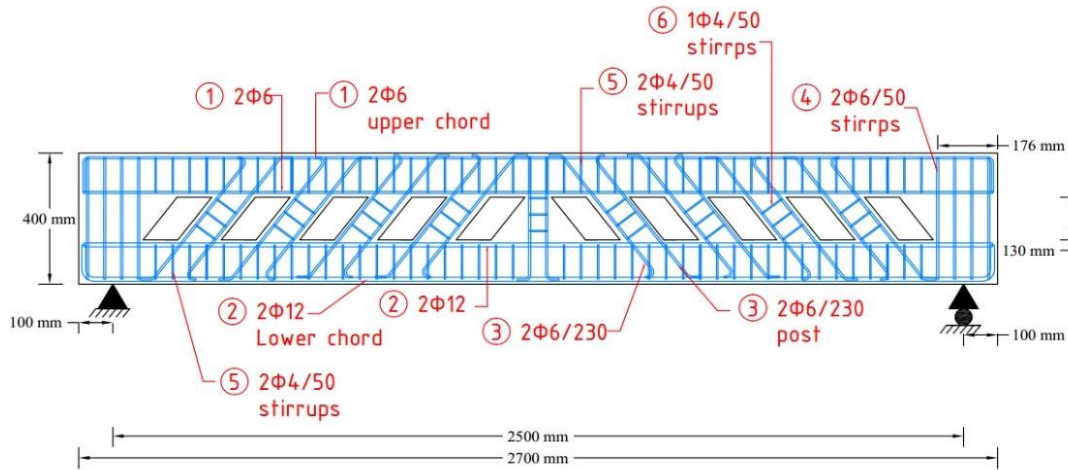


Figure 2. Steel reinforcement details for the beam with openings

Table 2. Materials properties

Material	Diameter (mm)	Yield stress (MPa)	Compressive strength for cube (MPa)	Compressive strength for cylinder (MPa)	Tensile strength (Mpa)
Concrete	-----	-----	37.56	30.799	2.36
steel	4	406	-----	-----	650
	6	390			445
	12	539			709

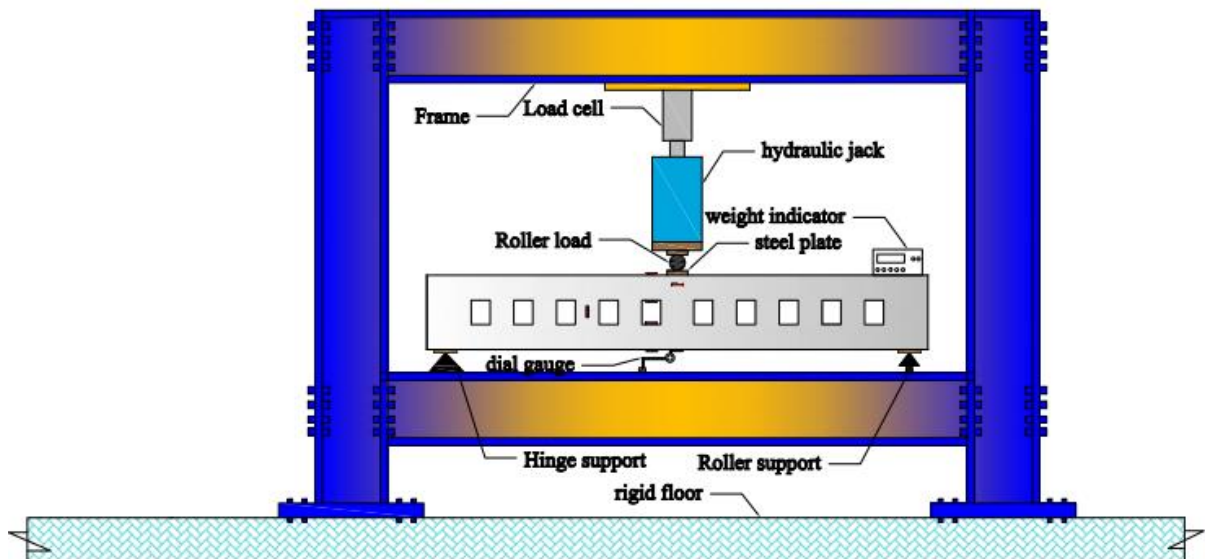


Figure 3. Details frame of the test

3. Finite element approach

3.1. Concrete and steel reinforcement modeling

Ten reinforced concrete beams with and without apertures were mathematically modeled using the ABAQUS standard finite element algorithm, which can tackle both linear and nonlinear problems. Concrete damage plasticity technique (CDP) is used to model inelastic concrete behavior. Table 3 lists the concrete damage plasticity parameters that were investigated in this investigation. The ABAQUS user handbook has more information on the concrete damage plasticity concept.

Table 3. Details of the parameter CDP

Parameter	Description	Value	Reference
(ψ)	Dilation angle: It is the internal friction angle of material or, in other words, the angle of the interaction of the surface failure to the hydrostatic axis.	30	[18]
(ϵ)	Eccentricity: It is the length of the segment between the interaction asymptotes of the hyperbola and the vertex of the hyperbola; alternatively, it is the ratio of tensile and compression strength.	0.1	[2]
$\frac{f_{bo}}{f_{co}}$	The biaxial compressive yield strength divided by the uniaxial compressive yield strength is the ratio.	1.16	[2]
K	In a deviatoric cross-section, it is the distance between the hydrostatic axis and the compression and tension meridian.	0.667	[2]
(μ)	Viscosity parameter: It is the relaxation time of a viscoelastic material system; otherwise, it is the time it takes for the material to respond to an increase in applied load.	0.0005	[19]

Compressive behavior of the concrete represented by stress-strain curve by using equations proposed by [2] and [20] to define compressive behavior in term of the compressive stress and inelastic strain are as follows figure 4.

$$\sigma_c = E_c \times \frac{\epsilon_c}{1 + \left(\frac{\epsilon_c}{\epsilon_o}\right)^2} \quad (1)$$

$$\epsilon_{oc}^{el} = \frac{\sigma_c}{E_c} \quad (2)$$

$$\epsilon_c^{\sim in} = \epsilon_c - \epsilon_{oc}^{el} \quad (3)$$

Where σ_c compressive stress at any compressive strain ϵ_c of the concrete, ϵ_o compressive strain at maximum compressive stress equal $\left(\frac{2f'_c}{E_c}\right)$, ϵ_{oc}^{el} the elastic strain of the concrete, $\epsilon_c^{\sim in}$ the concrete's inelastic strain and the concrete's elasticity modulus.

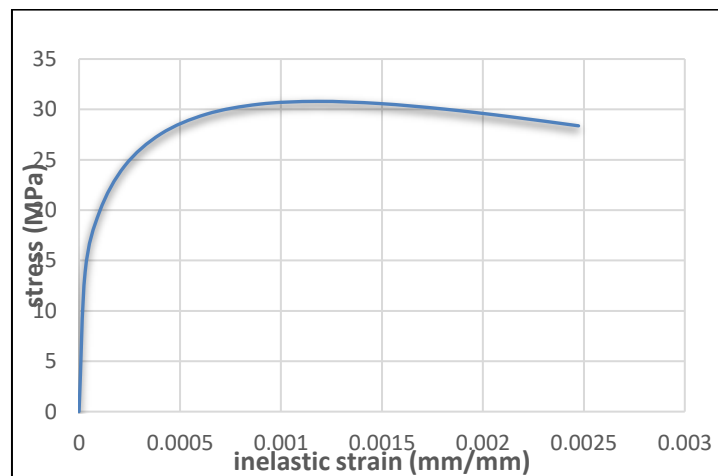


Figure 4. stress-inelastic strain curve for concrete compression behavior

Stiffness of degradations of compression behavior of the concrete and stiffness recovery under cycle loading were defined, because of the importance of the concrete's mechanical response in the CDP approach. Damage parameter of compression behavior of the concrete (d_c), is at the range between zero and one, which represented the material undamaged to total losses of load-bearing capacity ($0 < d_c < 1$), in other words, it is the ratio between stresses of the declining segment of the stress-inelastic strain curve in compressive behavior to the compressive strength of the concrete (f'_c), [2]The compression stiffness recovery (w_c), on the other hand, is recovered at crack closure as the load transitions from tension to compression; the ABAQUS user manual suggests using the default value ($w_c = 1$) [1].

$$d_c = 1 - \frac{\sigma_c}{f'_c} \tag{4}$$

Tension behavior of the concrete is defined in this study by using equations proposed by [2] and [21] to represent the tensile stress versus cracking strain which is illustrated in Figure (5).

$$\sigma_t = f_{cr} * \left(\frac{\varepsilon_{cr}}{\varepsilon_t}\right)^{0.4} \tag{5}$$

$$\varepsilon_{ot}^{el} = \frac{\varepsilon_t}{E_c} \tag{6}$$

$$\varepsilon_t^{ck} = \varepsilon_t - \varepsilon_{ot}^{el} \tag{7}$$

Where σ_t is the tensile stress of the concrete, f_{cr} modulus of rupture ($0.62 \sqrt{f'_c}$), ε_{cr} cracking strain at a maximum tensile stress of the concrete (0.00008 mm/mm), ε_t concrete tensile strain at any tensile stress σ_t of the concrete, ε_{ot}^{el} Elastic tensile strain (mm/mm) and ε_t^{ck} cracking strain at any tensile stress of the concrete σ_t (mm/mm). In the end, define the stiffness of degradation of the tension behavior of the concrete and stiffness recovery. Damage parameter of the tension behavior of the concrete (d_t) is the ratio between stresses for the declining segment of the stress-cracking strain curve in tensile behavior to cracking stress (strength of rupture f_{cr}), ranged at ($0 < d_t < 1$) [2]. From experimental observation in the materials have most quasi-brittle including concrete material, the tension stiffness (w_t) not recovered because of crashing micro-cracks have been developed, ABAQUS user manual recommended using the default value ($w_t = 0$) [1].

$$d_t = 1 - \frac{f_t}{f_{cr}} \tag{8}$$

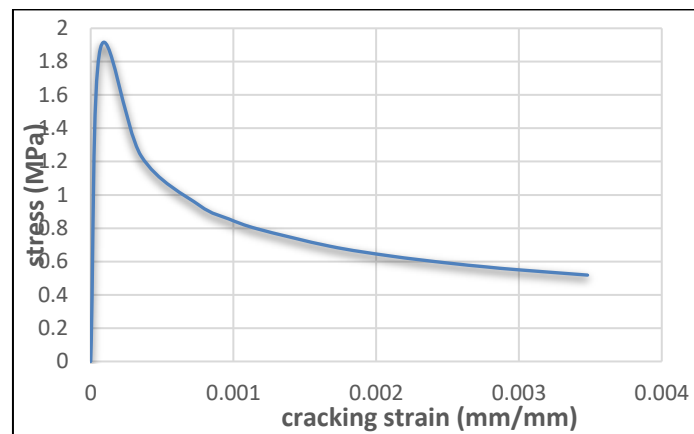


Figure 5. stress-cracking strain curve for concrete tensile behavior

To simulate the steel reinforcement behavior is adopted the bilinear model as shown in figure 6, depending on the Von mises failure concept, It takes into account the material's elastic nature until it reaches yield stress, after which it becomes totally flexible and shows no stiffness.

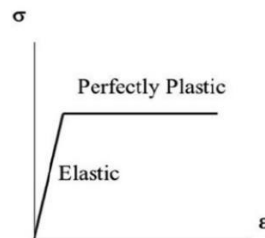


Figure 6. Bilinear Stress-strain curve of the steel reinforcement

3.2. Assemblage, boundary condition, and loading type

All concrete beams generated by using 3D model space and deformable type with base feature solid extrusion type, whereas the steel reinforcement used was wire planer type. The beams were sketched depending on the

configurations and sizes of openings. All concrete beams and steel reinforcement were assembled as dependent parts instance together in the global system as illustrated in Figure 7. The next interaction surface was created between steel reinforcement and whole concrete by using embedded region constraints.

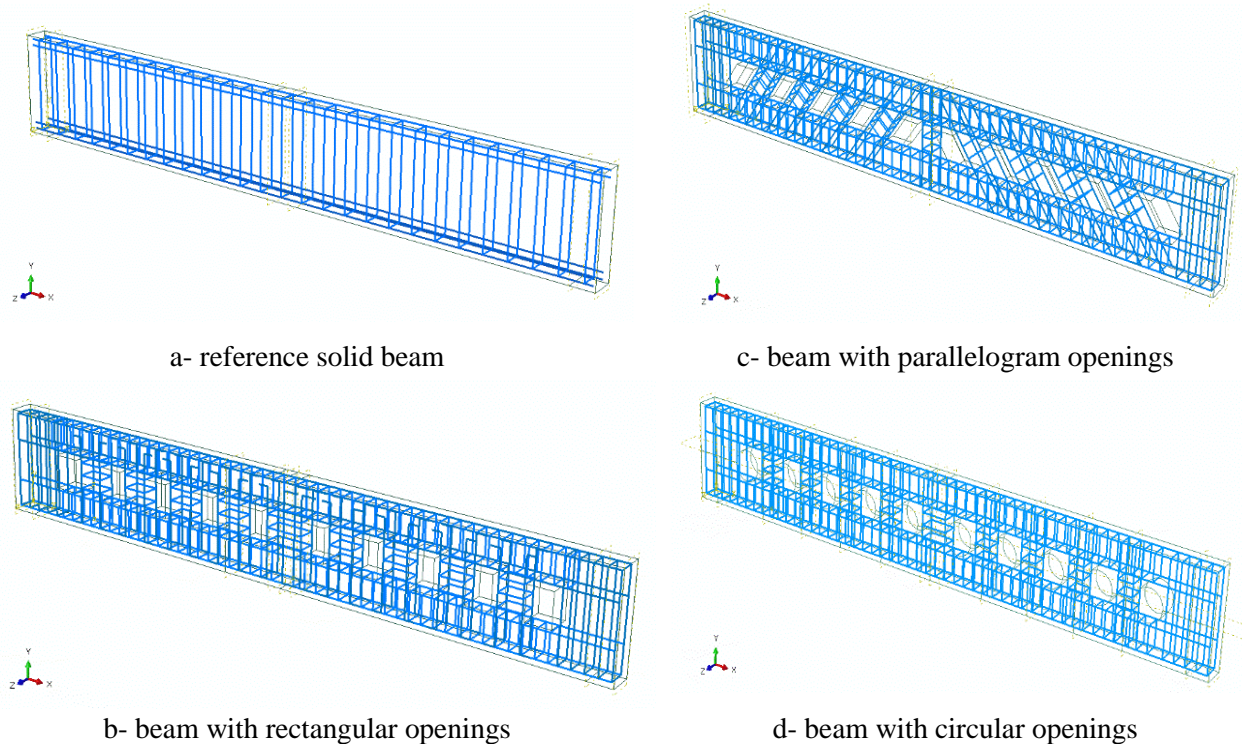


Figure 7. Assemblage concrete beams with steel reinforcement

A static general step procedure was used with the neglected effect of the inertia and time-dependent material to represent the displacement at the top face of the beam, while the initial step representing the boundary condition which constrains of the simply supported beam. Load and supports of the beam described according to the procedure of the analysis that selected previously. Applied load step, type (displacement/rotation), was used to represent displacement area of (100x100) mm at the top surface of the beam. Experimental work was employed to simulate concentrated load at mid-span, and displacement values of the beams with and without holes were determined. Whereas the first step, type (displacement/rotation), was used to represent the boundary condition of simply supports beam (ideal knife-edge support according to the approach of mechanics of materials), Supports were relocated at a distance using a hinge (i.e. $U_x = U_y = U_z = 0$) that allowed rotation about the x-axis and a roller (i.e. $U_y = U_z = 0$) that allowed longitudinal movement and rotation about the x-axis.

3.3. Meshing and analysis of the model

All models were generated by finite element mesh technique as shown in Figure (8), which has the approximate global size of 20 mm depending on the maximum size of aggregate (5-20) mm, which was used in the experimental work. Element type used family 3D stress 8-node line brick and hybrid with constant pressure and reduced integration of the concrete model (C3D8RH), while the steel reinforcement model used was 2-node linear with 3D truss (T3D2). Finally, the finite element approach allows configuring the analysis procedure required to accomplish the model by specifying increments (automatic or fixed increment). In this study was used static analysis with automatic step increments are utilized.

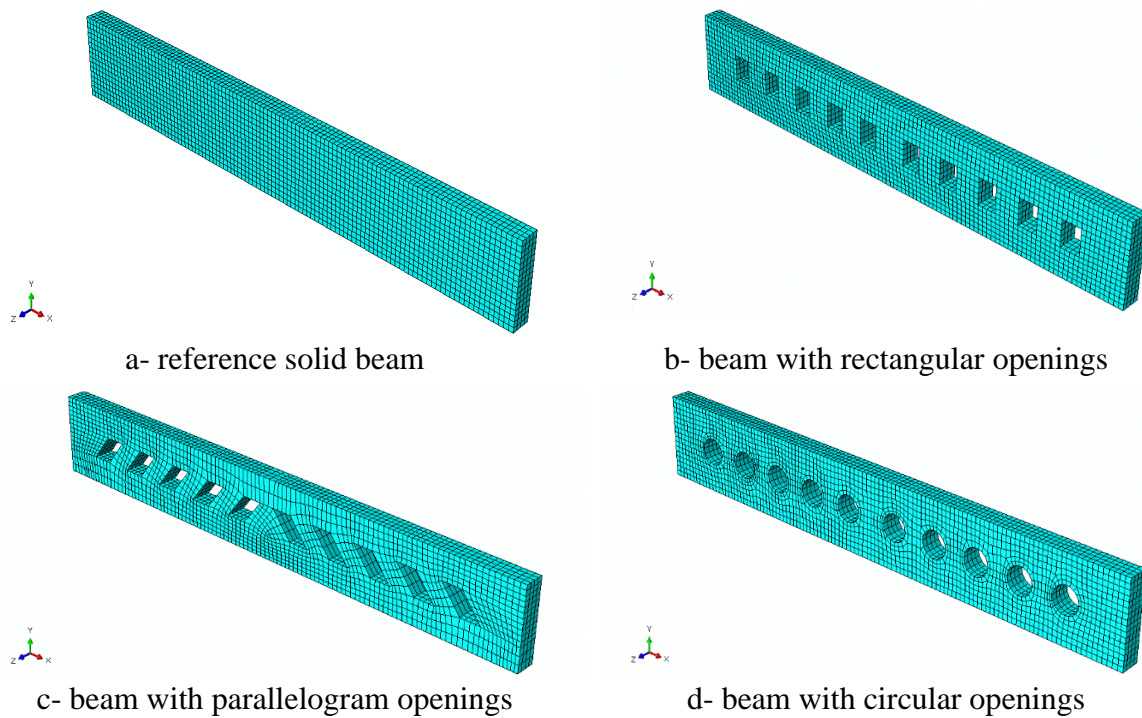


Figure 8. Numerically mesh of the beams

4. Finite element analysis results and discussion

4.1. Failure load

Numerically analysis results of the models reinforced concrete beams with and without openings are verify with experimental results of a load of the failure as listed in Table 4. The aim of the comparison is to ensure that all simulation processes including element type, material properties, and convergence criteria are correct and adequate. Numerically results revealed good agreement between finite element analysis and experimentally tested beams for the load of the failure P_{FE}/P_{EXP} , the average value was (94%). When compared to experimental data, numerical results demonstrate that beams with circular openings are more efficient than the other two designs (rectangular and parallelogram), and beams with 10 holes are better than beams with eight openings.

Table 4 Comparison load of the failure

Group number	beam mark	Load of Failure (Exp) KN	Load of Failure (FEM) KN	$(P_{FE.}/P_{EXP.})$
solid beam	BS	109.76	125	1.14
Group I	BR130	80.36	76.95	0.96
	BT130	83.3	83.53	1.00
	BC130	99.96	90.037	0.90
Group II	BR150	70.56	75.39	1.07
	BT150	90.16	83.78	0.93
	BC150	99.96	89.09	0.89
Group III	BR175	75.46	65.98	0.87
	BT175	80.36	67.57	0.84
	BC175	85.26	71.036	0.83
			Mean	0.94

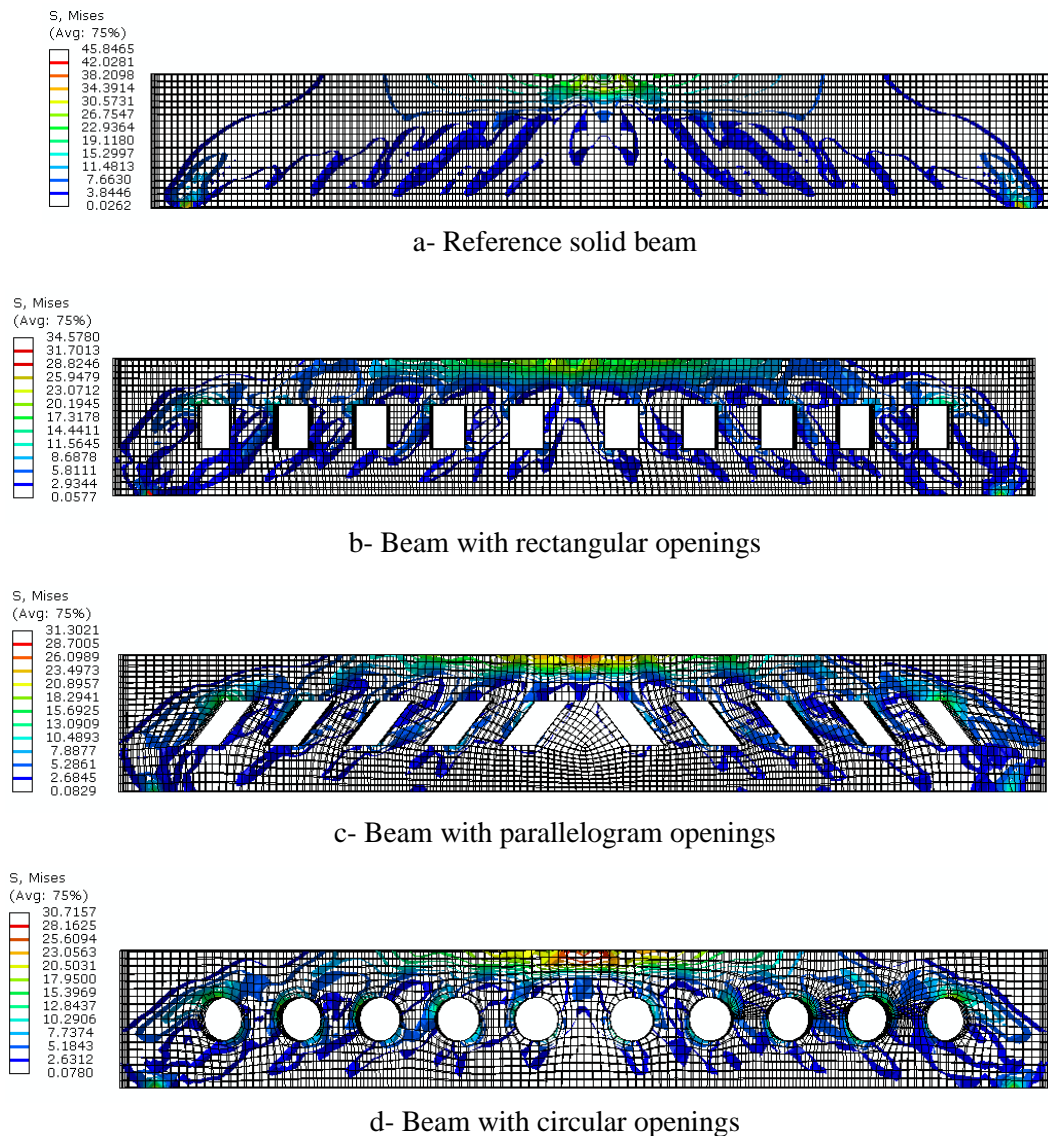


Figure 9. Stresses flow in the beams with and without openings

4.2. Stresses flow

The numerical analysis demonstrates octahedral shear stresses (Von Misses stresses), that led to failing almost of the materials as presented in Figure 9. From Figure, we notice distribution of the stresses in greater portions of the beams, that it is better than in case of the beams with a single opening. Illustration 9 Concentrated shear forces at the corners of the beams result in rectangular and parallelogram apertures due to shear failure of the posts of the beams. In contrast, stresses in beams with circular openings are evenly distributed across the opening. As a result, the circular opening beams outperform the other two designs. When comparing parallelogram and rectangular holes, however, the parallelogram openings were more efficient, likely due to the inclination of the posts with the direction of the stresses flow to the nearest support as opposed to the vertical one. Finally, stresses flow can help to predict the strut-tie truss model to design and analyze the beams with multiple openings.

4.3. Distribution of strains along beams with/without openings

Distribution and concentrated compressive and tensile strains at top fiber along the beams with/without openings at three loading stages as shown in the Figures 10 and 11. These figures demonstrate tensile strain at the ultimate stage, which causes plastic hinges at the ends of the upper chords because of Vierendeel action, also it reveals fluctuated in compressive strain because of drop-in beam stiffness compared to that reference solid beam, increased gradually up to the mid-span.

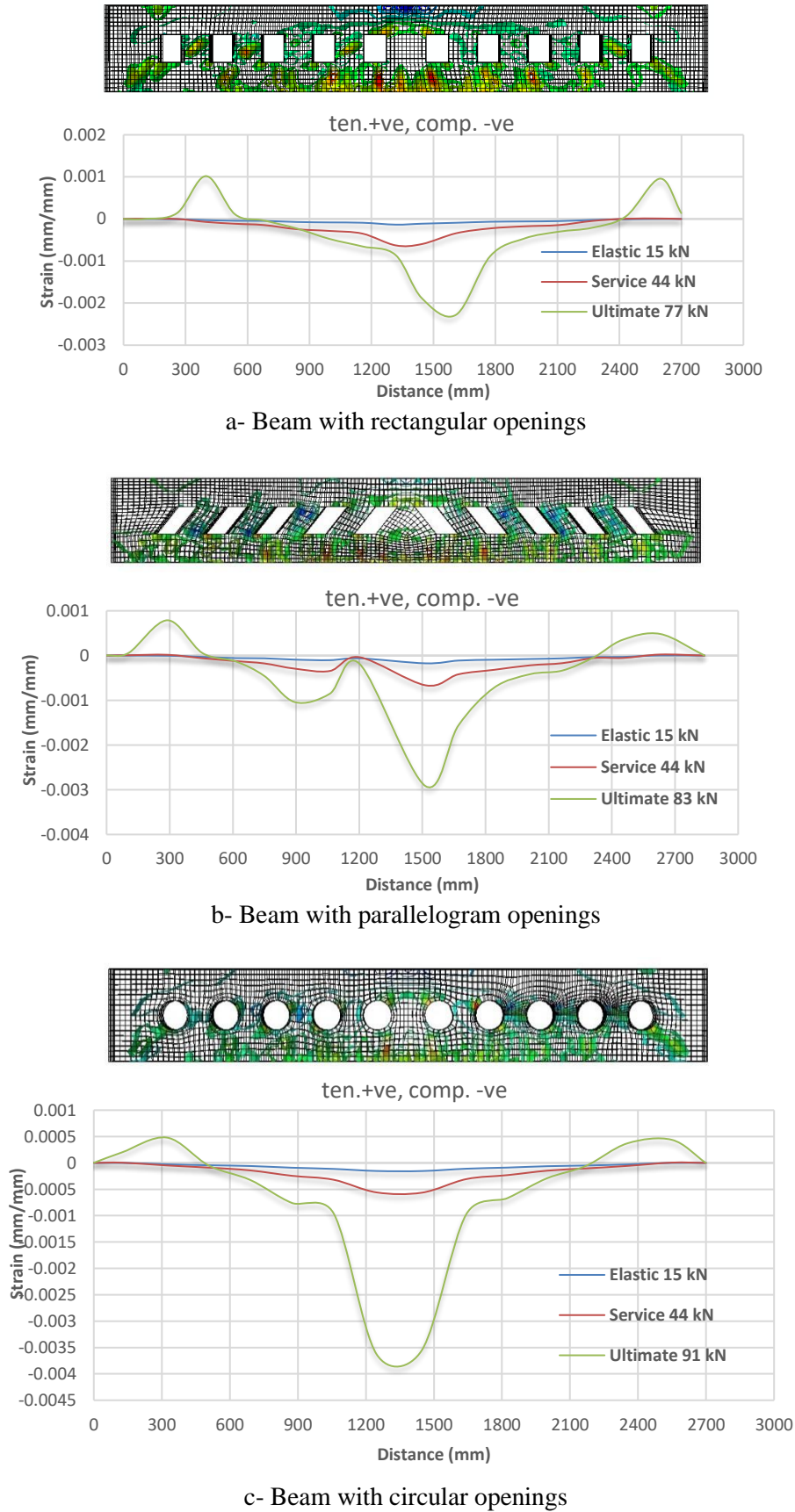


Figure 11 distribution of stains for beams with openings

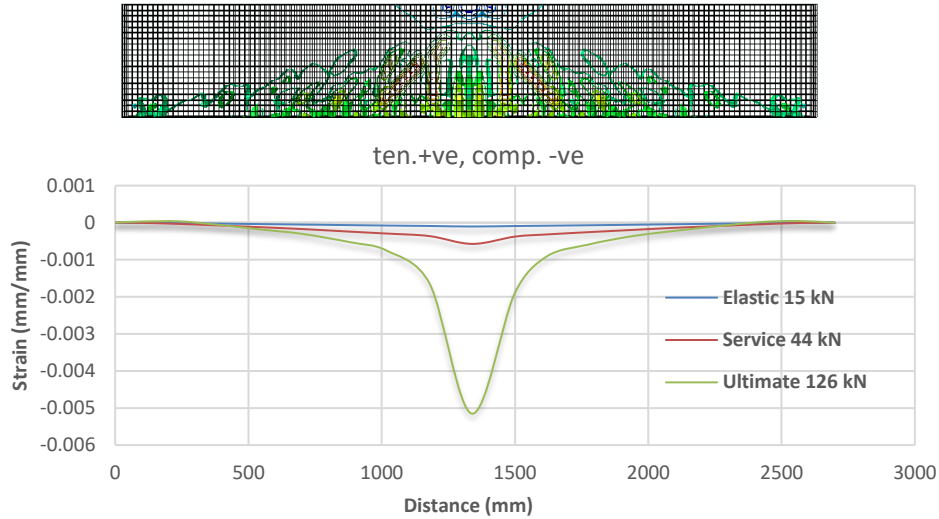


Figure 10. distribution of stains for reference solid beam

4.4. Influence of compressive strength and main longitudinal steel reinforcement

According to experimental and numerical analytical studies, the presence of openings in reinforced concrete beams lowered the load capacity of the beams. The following case studies have been proposed to recover the reduction in beam strength, including a 24 percent increase in concrete compressive strength (f_c) and a 28 percent and 44 percent increase in main longitudinal steel reinforcement (A_s) for beams of Groups I, as shown in Table (5).

Table 5 Details of the case study

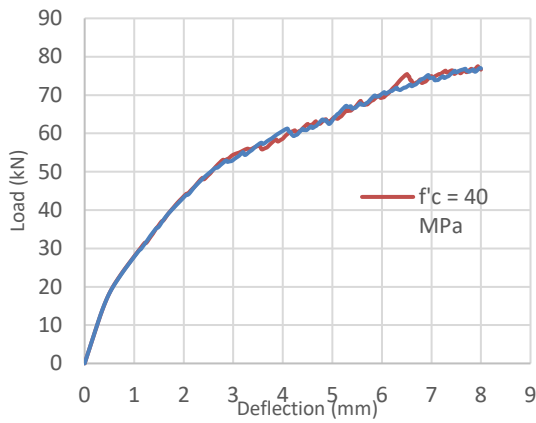
Case	Compressive strength (f_c) (MPa)	Increase %	Main Longitudinal Reinforcement	Area Steel (A_s) (mm ²)	Increase %
0	31	0	4Ø12	452	0
1	40	24	2Ø12&2Ø16	628	28
2	-	-	4Ø16	804	44

4.5. Influence of concrete compressive strength (f_c)

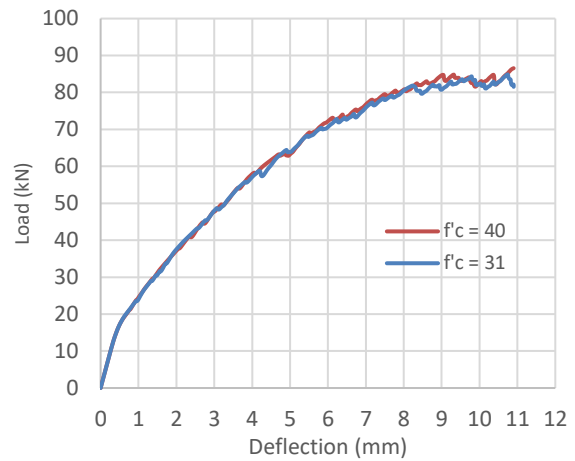
The effect of increasing concrete strength for beams with Group I apertures is listed in Table 6, and a comparison of load versus deflection of the beams is shown in Figure (12). The results revealed that raising compressive strength by 24 percent had a minor impact on the load capacity of the beams with apertures, increasing it by only 3.72 percent. The beam with rectangular openings (BR130) has a lower load capacity increase of 0.722 percent, 5.82 percent, and 4.62 percent, respectively, when compared to beams with parallelogram and circular openings (BT130 and BC130), indicating that beams with parallelogram and circular openings are more efficient than beams with rectangular openings.

Table 6. Load capacity for different compressive strength

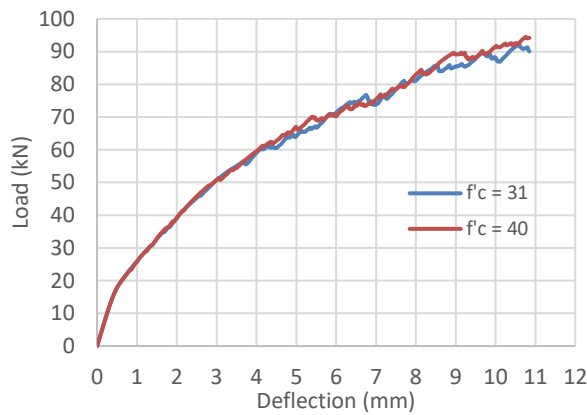
Group number	Beam designation	Ultimate Load at ($f_c = 31$ MPa) KN	Ultimate Load at ($f_c = 40$ MPa) KN	*Increasing %
Group I	BR130	76.95	77.51	0.72
	BT130	81.53	86.56	5.82
	BC130	90.04	94.4	4.62
			Mean	3.72



a- Load versus deflection of BR130



b- Load versus deflection BT130



c- Load versus deflection of BC130

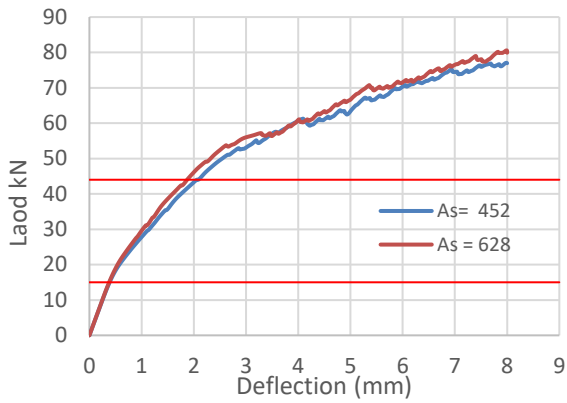
Figure 12. Influence of concrete strength on load-deflection of Group I

4.6. Influence of main steel reinforcement (As)

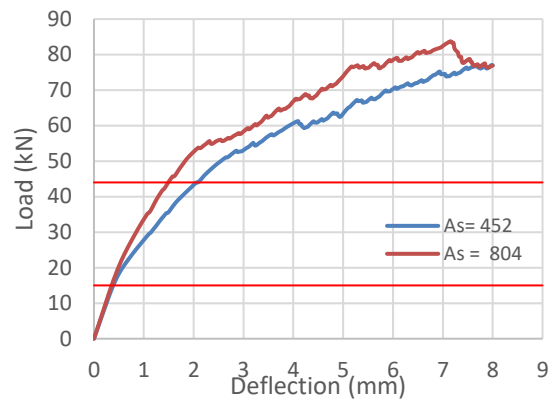
Table (7) depicts the numerical results of increasing the lower chord main steel reinforcement of beams with apertures, whereas Figure (13) depicts the load against deflection of these beams. Increased longitudinal steel reinforcement increased the load capacity of the beams with openings, according to the numerical results. The load capacity of the beams was raised by 7.61 percent and 9.61 percent, respectively, by adding 28 percent and 44 percent longitudinal steel reinforcement. As a result, the load capacity loss can be recovered by increasing primary longitudinal steel reinforcement while adhering to the ACI standards, and furthermore, additional reinforcements enhance the stiffness of the beams as illustrated in Figure (11). Numerical results indicate that the beam comprises rectangular openings (BR130) records higher enhancement compared with the other two configurations (BT130 and BC130) by increasing the main longitudinal steel reinforcement from 28% to 44%, which led to increasing the load capacity by rate 4.41% to 8.10% respectively. Whereas BT130 and BC130 led to an increase from 10.78% to 12.2% and 7.61% to 8.54%, respectively.

Table 6 Load capacity for different steel reinforcement

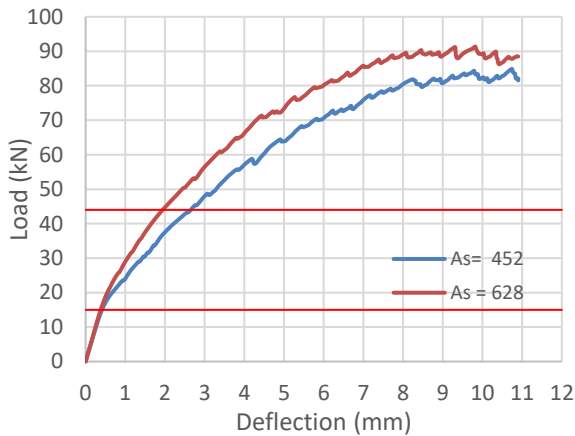
Group name	Beam designation	As ₀	As ₁		As ₂	
		Ultimate Load KN	Ultimate Load KN	Increasing* %	Ultimate Load KN	Increasing* %
Group I	BR130	76.95	80.5	4.41	83.73	8.10
	BT130	81.53	91.38	10.78	92.86	12.20
	BC130	90.04	97.45	7.61	98.44	8.54
			Mean	7.60	Mean	9.61



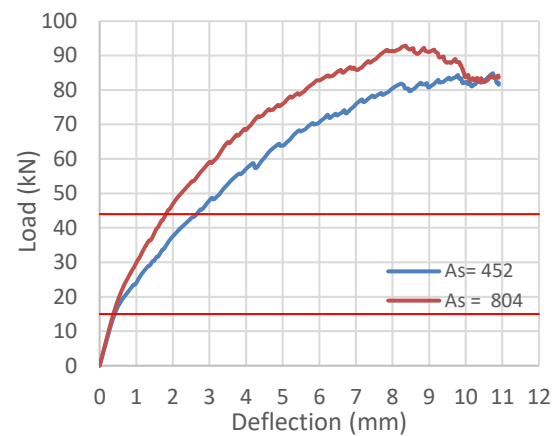
a- Load versus deflection of BR130 (case 1)



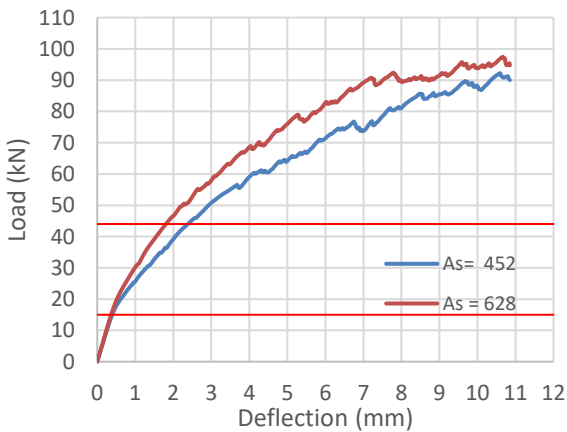
d- Load versus deflection of BR130 (case 2)



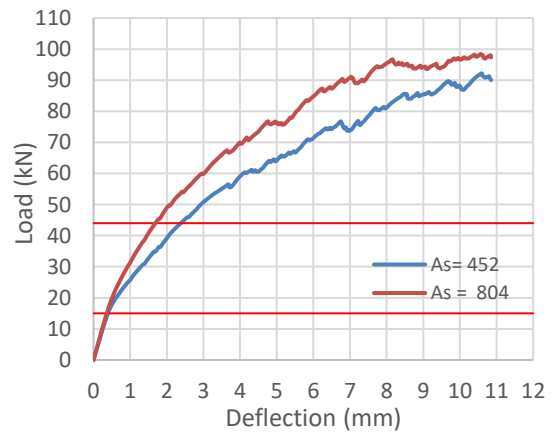
b- Load versus deflection of BT130 (case 1)



e- Load versus deflection of BT130 (case 2)



c- Load versus deflection of BC130 (case 1)



f- Load versus deflection of BC130 (case 2)

Figure 13 Influence of increasing main steel reinforcement on load-deflection curves of Group I

5. Conclusions

The numerical analytical study conclusions based on the modeling of reinforced concrete beams with multiple apertures, depending on the configurations and sizes of the openings, are as follows:

- 1- The failure load obtained from the experimental testing on ten reinforced concrete beams with/without apertures is 94 percent like the failure load derived from the finite element analysis. As a result, it is a very dependable and desired technique for analyzing the nonlinear behavior of beams with multiple apertures in terms of difficulty and time savings.

- 2- According to the findings, significant octahedral shear stresses exist at the corners of the openings (rectangular and parallelogram), hence the width of the posts between the openings should be considered throughout the design process. Furthermore, because stress distributions are uniformly distributed throughout the openings, beams with circular apertures were found to be more efficient than the other two configurations.
- 3- Finally, the numerical analysis shows that increasing longitudinal steel reinforcement by 28% and 44% with short stirrups in the chords effectively increased the ultimate load capacity of the beams with openings by 7.61 percent and 9.61 percent, respectively, when compared to increasing compressive strength of the beams by 24%, which resulted in an increase of 3.72 percent in ultimate load capacity.

Declaration of competing interest

The authors declare that they have no known financial or non-financial competing interests in any material discussed in this paper.

Funding information

No funding was received from any financial organization to conduct this research.

References

- [1] D.S.Simulia, Analysis User's Manual, USA, 2010.
- [2] M. P.Kmiecik, "Modelling of reinforced concrete structures and composite structures with concrete strength degradation taken into consideration," Archives of Civil Mechanical Engineering, pp. 623- 636, 2011.
- [3] H. K.W.Nasser, "Behavior and Design of Large Openings in Reinforced Concrete Beams," ACI Journal, pp. 25-33, 1967.
- [4] M.A.Mansur, A.Hasnat, "Concrete Beams with Small Openings Under Torsion," Journal of the Structural Division, pp. 2433-2447, 1979.
- [5] M.A.Mansur, K.H.Tan, S.L.Lee, "Design Method for Reinforced Concrete Beams with Large Openings," ACI Journal, pp. 517-524, 1985.
- [6] M.A.Mansur, Y.F.Lee, K.H.Tan, "Tests on RC Continuous Beams with Openings," Structural Engineering Journal, pp. 1593-1606, 1991.
- [7] M.A.Mansur., "Design of Reinforced Concrete Beams with Small Openings Under Combined Loading," ACI Journal, pp. 675-682, 1999.
- [8] N. A.-M.-B. I.A.S.Al-Shaarbaf, "Nonlinear Finite Element Analysis of Reinforced Concrete Beams with Large Openings under Flexure," Eng & Technology, pp. 210-228, 2005.
- [9] K. H.Madkhor, "Three-Dimension Modelling for Reinforced Concrete Beams with Openings Based on Nonlinear Elastic-Damage Theory," Journal of Engineering Sciences, pp. 9-27, 2007.
- [10] A. Sader Mohammed and L. Nasser Hussain, "Finite Element Modeling for Self-Compacting Reinforced Concrete Deep Beams Containing Web Openings," International Journal of Engineering & Technology, vol. 7, no. 4.20, p. 546, Nov. 2018.
- [11] H. E. J. A.-K. A. Shubbar, "Studying the Structural Behavior of RC Beams with Circular Openings of Different Size and Locations using FE Method," International Journal of Civil, Environmental, Structural, Construction, and Architectural Engineering, vol. 11, pp. 849-852, 2017.
- [12] K. F. El-Kashif, "Computational Model of Ultimate Capacity and Behavior of Reinforced Concrete Beams with Multiple Openings," Al-Azhar University Civil Engineering Research Magazine, pp. 249-267, 2018.
- [13] M.A.J.Hassan, "Finite element modeling of RC gable roof beams with openings of different sizes and configurations," Mechanics of Advanced Materials and Structures, pp. 2-17, 2019.
- [14] British Standard Institution, "Testing Concrete-Part 116:Method for Determination of Compressive Strength of Concrete Cubes," 1998.

- [15] ASTM, C496M-11, "Standard Test Method for Splitting Tensile Strength of Cylindrical Concrete Specimens", West Conshohocken- the United States, 2011.
- [16] ASTM, C39/C39M-15a, "Standard Test Method for Compressive Strength of Cylindrical Concrete Specimens", West Conshohocken- the United States, 2015.
- [17] ASTM, A615/615M-15a, Standard Specification for Deformed and Plain Carbon-Steel Bars for Concrete Reinforcement, West Conshohocken- the United States, 2015.
- [18] M. R.N.Hamedani, Numerical Evaluation of Structural Behavior of the Simply Supported FRP-RC Beams, Stockholm, Sweden, 2012.
- [19] H. K. M. A. A.Demir, "Effect of Viscosity Parameter on the Numerical Simulation of Reinforced Concrete Deep Beam Behavior," The Online Journal of Science and Technology, pp. pp. 50- 56, 2018.
- [20] P. S.Krishnan, "Equation for Stress-Strain Curve of Concrete," Journal of the American Concrete Institute, pp. pp. 345- 350, 1964.
- [21] T. A.Belarbi, "Constitutive Laws of Concrete in Tension and Reinforcing Bars Stiffened by Concrete," ACI Structural Journal, pp. pp.465- 474, 1994.